Near-Optimal Quantization for LoS MIMO with QPSK Modulation

Ahmet Dundar Sezer and Upamanyu Madhow
Department of Electrical and Computer Engineering
University of California, Santa Barbara
Santa Barbara, California 93106
Email: {adsezer, madhow}@ece.ucsb.edu

***Abstract*—As signaling bandwidths increase, analog-to-digital conversion becomes a fundamental bottleneck for modern all-digital baseband signal processing architectures. Motivated by emerging millimeter (mm) wave communication systems, we investigate the impact of severe quantization for 2×2 and 4×4 line-of-sight (LoS) multi-input and multi-output (MIMO) systems employing QPSK. Unlike prior work on MIMO with low-precision quantization, channel state information is utilized only at the receiver (i.e., transmit precoding is not employed). Rather than designing an optimal quantizer, we focus on quantizers with regular structure, and ask whether high-SNR performance approaches that of an unquantized system. First, we prove for a 2×2 MIMO system that phase-only quantization (attractive because it does not require automatic gain control) is unable to achieve this, but that 2-level amplitude and 8-level phase quantization can achieve the maximum data rate of 4 bits per channel use as SNR gets large. We then show that quantizer design based on conventional minimum mean squared quantization error (MMSQE) criterion performs worse than a quantizer based on equal-probability regions. We show that I/Q quantization with 16 regions per antenna using the equal probability criterion achieves the unquantized benchmark at high SNR, which is a maximum data rate of 8 bits per channel use. We illustrate our investigations via numerical examples.**

I. Introduction

Modern communication receivers employ all-digital signal processing, with baseband signals converted to the digital domain with analog-to-digital converters (ADCs), typically with precisions of 8-12 bits per real-valued sample. As signaling bandwidths increase, however, realizing high-precision ADCs becomes a challenge [1]. This could be addressed, for example, by hybrid analog/digital processing (with analog processing typically used to reduce dynamic range prior to quantization), but all-digital processing with severely quantized samples is an attractive alternative. In this paper, we investigate the latter approach for system models motivated by emerging millimeter (mm) wave applications: 2×2 and 4×4 LoS MIMO [2] systems employing QPSK modulation over each data stream, resulting in a maximum data rate of, respectively, 4 bits and 8 bits per channel use. Such a setting is particularly attractive for exploring the feasibility of attaining good performance with drastic quantization, since small constellations and a simple channel result in a relatively small dynamic range for the received signal.

Contributions: Rather than trying to design optimal quantizers, our goal is to design quantizers with regular structure which approach the same Shannon limit as an unquantized system at high SNR. A particularly attractive approach is phase-only quantization: this can be implemented by passing linear combinations of the real and imaginary parts of the sample through sign detectors (one-bit ADCs), and therefore does not require automatic gain control. Our main results are as follows:

For a 2×2 LoS MIMO system:
(1) We prove that phase-only quantizers do not meet the unquantized benchmark at high SNR.
(2) We prove that 2-level amplitude and 8-level phase quantization does meet the unquantized benchmark at high SNR, thus demonstrating the necessity for amplitude quantization for achieving the unquantized benchmark at high SNR.

For a 4×4 LoS MIMO system:
(1) We show that per-antenna quantization into equal probability regions performs better than conventional MMSE quantization, and that I/Q quantization performs better than amplitude/phase quantization.
(2) We show that I/Q quantization designed based on 16 equal probability regions can achieve the unquantized benchmark at high SNR, attaining a maximum data rate of 8 bits per channel use.

Related work: Shannon limits for an ideal SISO discrete-time additive white Gaussian noise (AWGN) channel with low-precision ADC are studied in [3]. It is shown that the optimal input distribution is discrete and can be computed numerically, but standard constellations are near-optimal. Further, the use of ADCs with 2-3 bits precision results in only a small reduction in channel capacity even at moderately high SNR. Our model is perhaps the simplest possible extension of this framework to MIMO systems.

Prior work on MIMO capacity with low-precision ADC assumes that the transmitter performs precoding, utilizing channel state information. The channel capacity with 1-bit ADC is studied in [4], which provides capacity bounds and a convex optimization based algorithm to obtain capacity-achieving constellations. In [5], the capacity with transmit precoding, together with hybrid analog-digital processing at the receiver, where analog linear combinations of the signals received at different antennas are quantized, is studied. In our system model, we avoid transmit precoding, since the increased dynamic range aggravates the already difficult problem of producing power at millimeter wave frequencies.

Prior research on LoS MIMO implementations in the setting considered here explores the feasibility of analog-centric spatial demultiplexing [6] and [7] which sidesteps the ADC bottleneck as bandwidths scale up. LoS MIMO with digital reception has been implemented in industry, but to the best of our knowledge, employs standard precision ADCs rather than pushing the limits of low precision as in this paper.

We assume that the receiver has ideal channel estimates. Channel estimation with low-precision ADC is not as challenging as demodulation: [8] is an early example for a SISO dispersive channel, while [9] proposes effective estimation techniques for massive MIMO with 1-bit quantization at the receive antennas.

Notation: Throughout the paper, random variables are denoted by capital letters and small letters are used for the specific value that the random variables take. Bold letters are used to denote vectors and matrices. $\mathbb{E}_Z$ denotes the expectation operator over the random variable Z. $|Z|$ and $\angle Z$ represent the amplitude and the phase of Z, respectively. $\mathbf{X}^\intercal$ and $\mathbf{X}^\dagger$ are the transpose and Hermitian transpose of $\mathbf{X}$, respectively. $\mathbf{I}_n$ is the identity matrix of size n.

II. System Model and Problem Formulation

Consider a 2×2 LoS MIMO communication scheme in which two transmit antennas (i.e., $N_T = 2$) are aligned with two receive antennas (i.e., $N_R = 2$) with inter-antenna spacing of d and horizontal distance of R as illustrated in Fig. 1. Each transmit/receive antenna (which may itself be a "subarray" [2]) forms a highly directive beam along the LoS, and multipath is ignored. The received signal vector $\mathbf{Y} \triangleq [Y_1\, Y_2]^\intercal \in \mathbb{C}^{2\times 1}$ is given by

$$\mathbf{Y} = \mathbf{H}\,\mathbf{X} + \mathbf{N}\,, \tag{1}$$

where $\mathbf{X} \triangleq [X_1\, X_2]^\intercal \in \mathbb{C}^{2\times 1}$ is the transmitted symbol vector, $\mathbf{H} \in \mathbb{C}^{2\times 2}$ is the channel matrix, and $\mathbf{N} \sim \mathcal{CN}(0, \sigma^2\,\mathbf{I}_2)$ is AWGN. Since the path loss differences among the transmitters and the receivers are negligible, the normalized channel matrix is given by

$$\mathbf{H} = \frac{1}{\sqrt{2}} e^{j\Phi} \begin{bmatrix} 1 & e^{j\theta} \\ e^{j\theta} & 1 \end{bmatrix}, \tag{2}$$

where the random variable Φ denotes the common phase change along the path between the transmitter and the receiver and $\theta \approx \frac{\pi d^2}{\lambda R}$ for $R \gg d$ with λ indicating the carrier wavelength. We would like our quantizer designs to be robust to variations in Φ, which is assumed to be uniformly distributed over $[0, 2\pi)$.

The quantized output of the ith receive antenna can be expressed as

$$\bar{Y}_i = Q^{(i)}(Y_i)\,, \tag{3}$$

for $i \in \{1, \ldots, N_R\}$. $Q^{(i)}(\cdot)$ in (3) represents the quantizer function at the ith receive antenna and for a given input y, $Q^{(i)}(y)$ can be characterized as

$$Q^{(i)}(y) = j\,, \text{ if } \; y \in \Gamma_j^{(i)}\,, \tag{4}$$

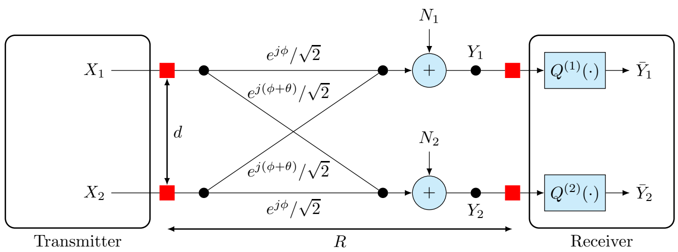

Fig. 1. 2×2 LoS MIMO communication system model

for $j \in \{1, \ldots, K_i\}$, where $\Gamma_1^{(i)}, \ldots, \Gamma_{K_i}^{(i)}$ denote the decision regions for the quantizer, with K_i denoting the number of quantizer bins at the ith receive antenna.

For QPSK modulation, $\{X_i\}_{i=1}^{N_T}$ are independent and identically distributed symbols taking values $\{e^{j\pi/4}, e^{j3\pi/4}, e^{j5\pi/4}, e^{j7\pi/4}\}$ with equal probability. We define $SNR = \mathbb{E}\{|X_k|^2\}/\sigma^2 = 1/\sigma^2$ where $\mathbb{E}\{|X_k|^2\} = 1$ for all $k \in \{1, \ldots, N_T\}$.

One possible formulation of optimal quantization is to minimize

$$D(\mathbf{X}, \mathbf{Y}_Q, \theta) \triangleq \mathbb{E}_\Phi\{I(\mathbf{X}; \mathbf{Y} \mid \Phi, \theta) - I(\mathbf{X}; \mathbf{Y}_Q \mid \Phi, \theta)\} \tag{5}$$

where $\mathbf{Y}_Q \triangleq \left[\bar{Y}_1\, \bar{Y}_2\right]^\intercal$ and the function $I(\bar{\mathbf{X}}; \bar{\mathbf{Y}} \mid \Phi, \theta)$ represents the mutual information between the random variables $\bar{\mathbf{X}}$ and $\bar{\mathbf{Y}}$ for given Φ and θ. Based on the data processing equality, $D(\mathbf{X}, \mathbf{Y}_Q, \theta) \geq 0$ since $\mathbf{X}$, $\mathbf{Y}$, and $\mathbf{Y}_Q$ form a Markov chain; that is, $\mathbf{X} \to \mathbf{Y} \to \mathbf{Y}_Q$. Also, $I(\mathbf{X}; \mathbf{Y} \mid \Phi, \theta)$ in (5) does not depend on any parameter related to quantizer. For that reason, the problem of minimizing $D(\mathbf{X}, \mathbf{Y}_Q, \theta)$ in (5) is equivalent to

$$\max_{\{\{\Gamma_j^{(i)}\}_{j=1}^{K_i}\}_{i=1}^{2}} \mathbb{E}_\Phi\{I(\mathbf{X}; \mathbf{Y}_Q \mid \Phi, \theta)\}\,. \tag{6}$$

In the optimization problem in (6), the mutual information between $\mathbf{X}$ and $\mathbf{Y}_Q$ must be maximized over the set of all possible quantization regions of the quantizers at the receive antennas. The number of quantization bins for each quantizer is not fixed in (6), and must also be optimized. Thus, it is difficult to solve (6). Furthermore, the optimal quantizers may correspond to irregular regions, leading to implementation difficulties. In this paper, therefore, we opt for designing regular quantizers with the goal of ensuring that $D(\mathbf{X}, \mathbf{Y}_Q, \theta) \to 0$ at high SNR.

III. Phase-only Quantization

In this section, we consider M-ary phase-only quantization with $Q^{(1)} = Q^{(2)}$. Let $\{\bar{\Gamma}_i\}_{i=1}^{M}$ denote the equally partitioned quantization regions of the phase-only quantizers at the receivers. Then, the quantization set of ith-bin (i.e., ith-sector) can be expressed as

$$\bar{\Gamma}_i = \{\bar{Y} \mid \frac{2\pi}{M}(i-1) \leq \angle\bar{Y} < \frac{2\pi}{M} i\}\,, \tag{7}$$

for $i \in \{1, \ldots, M\}$. Our goal is to determine whether such a scheme attains the unquantized benchmark, and the number of bins required for adequate performance.

The following lemma establishes a negative result: for some pairs of $\mathbf{X}$, the noise-free outputs prior to quantization have the same phase value. Thus, when phase-only quantization is considered, those outputs reside in the same quantization bin and consequently cannot be distinguished by using any possible phase-only quantization scheme.

Lemma 1: *Suppose* $Y_1^{(i)} \triangleq e^{j\phi}(X_1^{(i)} + e^{j\theta}X_2^{(i)})/\sqrt{2}$ *and* $Y_2^{(i)} \triangleq e^{j\phi}(e^{j\theta}X_1^{(i)} + X_2^{(i)})/\sqrt{2}$ *for* $i \in \{1, 2\}$. *For* $(X_1^{(1)}, X_2^{(1)}) = (e^{j\pi(2i-1)/4}, e^{j\pi(2i+1)/4})$ *where* $i \in \{1, \ldots, 4\}$, *the following statements holds:*

(i) For $\theta \in (-\pi/2, \pi/2)$ *and* $(X_1^{(2)}, X_2^{(2)}) = (X_2^{(1)}, X_1^{(1)})$,

$$\angle Y_1^{(1)} = \angle Y_2^{(1)} \tag{8}$$
$$\angle Y_1^{(2)} = \angle Y_2^{(2)} \tag{9}$$
$$\angle Y_1^{(1)} = \angle Y_1^{(2)} \tag{10}$$

(ii) For $\theta \in (\pi/2, 3\pi/2)$ *and* $(X_1^{(2)}, X_2^{(2)}) = (X_2^{(1)}, X_1^{(1)})$,

$$\angle Y_1^{(1)} = \angle Y_2^{(1)} + \pi \tag{11}$$
$$\angle Y_1^{(2)} = \angle Y_2^{(2)} + \pi \tag{12}$$
$$\angle Y_1^{(1)} = \angle Y_1^{(2)} + \pi \tag{13}$$

(iii) For $\theta \in (-\pi/2, \pi/2)$ *and* $(X_1^{(2)}, X_2^{(2)}) = (e^{j\pi}X_2^{(1)}, e^{j\pi}X_1^{(1)})$,

$$\angle Y_1^{(1)} = \angle Y_2^{(1)} \tag{14}$$
$$\angle Y_1^{(2)} = \angle Y_2^{(2)} \tag{15}$$
$$\angle Y_1^{(1)} = \angle Y_1^{(2)} + \pi \tag{16}$$

(iv) For $\theta \in (\pi/2, 3\pi/2)$ *and* $(X_1^{(2)}, X_2^{(2)}) = (e^{j\pi}X_2^{(1)}, e^{j\pi}X_1^{(1)})$,

$$\angle Y_1^{(1)} = \angle Y_2^{(1)} + \pi \tag{17}$$
$$\angle Y_1^{(2)} = \angle Y_2^{(2)} + \pi \tag{18}$$
$$\angle Y_1^{(1)} = \angle Y_1^{(2)} \tag{19}$$

Proof: The result in the lemma can simply be shown by using Euler's formula and Pythagorean trigonometric identity. ∎

This results in the following proposition stating that phase-only quantization cannot achieve the unquantized benchmark. The proposition is intuitively obvious from Lemma 1, hence we skip its proof.

Proposition 1: *For any phase-only quantization scheme with any number of bins,* $D(\mathbf{X}, \mathbf{Y}_Q, \theta) > 0$ *for all* $\theta \in [0, 2\pi)$ *as* $\sigma \to 0$.

Remark: We assume identical quantizers at both receive antennas for simplicity of exposition, but our negative result does not require this, and holds for any phase-only quantization scheme.

While the unquantized benchmark cannot be achieved, it is still of interest to ask how many phase quantization bins are enough to reach the high-SNR asymptote for phase-only quantization. We now establish that, for our system, 8 phase quantization bins suffice. We begin with the following lemma.

Lemma 2: *For any possible* $(X_1^{(1)}, X_2^{(1)})$ *and* $(X_1^{(2)}, X_2^{(2)})$ *input pairs,* $\angle Y_1^{(1)} - \angle Y_1^{(2)} = 0 \pmod{\pi/4}$ *and* $\angle Y_2^{(1)} - \angle Y_2^{(2)} = 0 \pmod{\pi/4}$, *where* $Y_1^{(i)}$ *and* $Y_2^{(i)}$ *are as defined in Lemma 1. Also,* $\angle Y_1^{(1)} - \angle Y_1^{(2)}$ *and* $\angle Y_2^{(1)} - \angle Y_2^{(2)}$ *can take* 8 *different values.*

Proof: By using $\arctan(x) - \arctan(y) = \arctan(\frac{x-y}{1+xy})$ and Euler's formula, the proof is straightforward. ∎

Based on Lemma 2, we can derive the following proposition stating that 8 phase quantization bins suffice. We skip its proof due to space limitation.

Proposition 2: *As* $\sigma \to 0$, *any phase-only quantization schemes with more than 8 regions cannot achieve higher data rate than phase-only quantization scheme with 8 equally partitioned sectors.*

IV. Amplitude and Phase Quantization

For K-ary amplitude and M-ary phase quantization, the quantization set of $(m + M(k-1))$th-bin of a quantizer can be written as

$$\bar{\Gamma}_{m+M(k-1)} = \{\bar{Y} \mid A_{k-1} \leq |\bar{Y}| < A_k\,, \quad \frac{2\pi}{M}(m-1) \leq \angle\bar{Y} < \frac{2\pi}{M}m\}\,, \tag{20}$$

for $m \in \{1, \ldots, M\}$ and $k \in \{1, \ldots, K\}$, where $A_1, \ldots, A_{K-1}$ are the amplitude thresholds (we set $A_0 = 0$ and $A_K = \infty$ to maintain a unified notation across quantization bins).

The following proposition states that $K = 2$ and $M = 8$ suffices to attain the unquantized benchmark.

Proposition 3: *As* $\sigma \to 0$, *a circularly symmetric quantization scheme with* 2*-level amplitude and* 8*-level phase quantization attains* $D(\mathbf{X}, \mathbf{Y}_Q, \theta) \to 0$ *for* $\theta \in [0, 2\pi)$.

Proof: Proposition 1 is based on the observation that the outputs of some input pairs have the same phase at both of the antennas as $\sigma \to 0$, so that those outputs cannot be differentiated by employing any phase-only quantization scheme. On the other hand, the proof of Proposition 2 shows that a phase-only scheme with equally partitioned 8 regions can distinguish noise-free outputs having two different phases, due to the result in Lemma 2. In this proof, the aim is to show that considering a 2-level amplitude quantization together with phase quantization resolves the ambiguities leading to the result in Proposition 1. First, it can be shown that only the outputs corresponding to the input pairs discussed in Lemma 1 cannot be distinguished via phase-only scheme having equally partitioned 8 regions. For that reason, consider the input pairs in Lemma 1. For $(X_1^{(1)}, X_2^{(1)}) = (e^{j\pi(2i-1)/4}, e^{j\pi(2i+1)/4})$ and $(X_1^{(2)}, X_2^{(2)}) = (X_2^{(1)}, X_1^{(1)})$, where $i \in \{1, \ldots, 4\}$, $|Y_1^{(1)}| < 1 < |Y_1^{(2)}|$ and $|Y_2^{(2)}| < 1 < |Y_2^{(1)}|$ for $\theta \in (0, \pi/2]$, $|Y_1^{(1)}| = |Y_1^{(2)}| = 1$ and

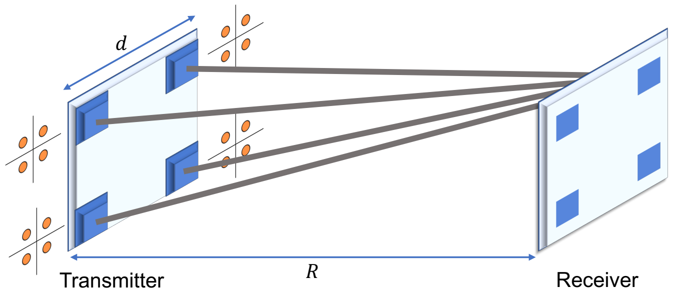

Fig. 2. 4×4 LoS MIMO communication system model

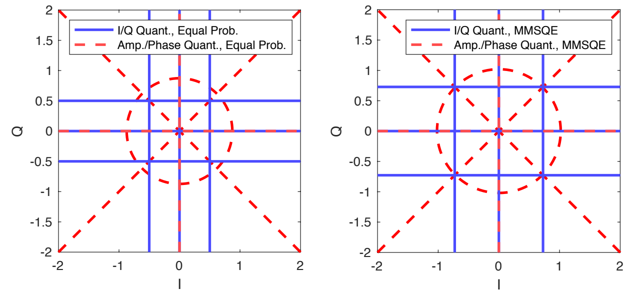

Fig. 3. Quantization schemes for 4×4 LoS MIMO at 10 dB SNR

$|Y_2^{(2)}| = |Y_2^{(1)}| = 1$ for $\theta = 0$, and $|Y_1^{(2)}| < 1 < |Y_1^{(1)}|$ and $|Y_2^{(1)}| < 1 < |Y_2^{(2)}|$ for $\theta \in [-\pi/2, 0)$. Due to the symmetry, the same approach can be applied for other input pairs (i.e., $(X_1^{(1)}, X_2^{(1)}) = (e^{j\pi(2i-1)/4}, e^{j\pi(2i+1)/4})$ and $(X_1^{(2)}, X_2^{(2)}) = (e^{j\pi}X_2^{(1)}, e^{j\pi}X_1^{(1)})$ for $i \in \{1, \ldots, 4\}$) when $\theta \in (\pi/2, 3\pi/2)$. Since the amplitude of the outputs does not depend on $\Phi = \phi$ and a circularly symmetric quantization scheme is employed, a phase quantization scheme including a 2-level amplitude quantization with $A_0 = 0$, $A_1 = 1$, and $A_2 = \infty$ resolves the ambiguity between those outputs. It is easy to now conclude that $D(\mathbf{X}, \mathbf{Y}_Q, \theta) \to 0$ for $\theta \in [0, 2\pi)$ as $\sigma \to 0$. ■

V. Quantization for 4×4 LoS MIMO

In this section, we extend our results to 4×4 LoS MIMO systems and obtain the regular quantizers for such systems. For that reason, consider a 4×4 LOS MIMO communication scheme in which 4 transmit and 4 receive antennas (i.e., $N_T = N_R = 4$) are configured in a two-dimensional (2D) planar array as in Fig. 2. For this scheme, $\mathbf{X}$ and $\mathbf{Y}$ in (1) are defined as $\mathbf{X} \triangleq [X_1\, X_2\, X_3\, X_4]^{\intercal} \in \mathbb{C}^{4\times1}$ and $\mathbf{Y} \triangleq [Y_1\, Y_2\, Y_3\, Y_4]^{\intercal} \in \mathbb{C}^{4\times1}$, respectively. Also, $\mathbf{N} \sim \mathcal{CN}(0, \sigma^2\, \mathbf{I}_4)$ and the normalized channel matrix for this scheme is given by

$$\mathbf{H} = \frac{1}{2}e^{j\Phi}\begin{bmatrix} 1 & e^{j\theta} & e^{j2\theta} & e^{j\theta} \\ e^{j\theta} & 1 & e^{j\theta} & e^{j2\theta} \\ e^{j2\theta} & e^{j\theta} & 1 & e^{j\theta} \\ e^{j\theta} & e^{j2\theta} & e^{j\theta} & 1 \end{bmatrix}. \tag{21}$$

In addition, $\mathbf{Y}_Q$ in (5) is defined by $\mathbf{Y}_Q \triangleq [\bar{Y}_1\, \bar{Y}_2\, \bar{Y}_3\, \bar{Y}_4]^{\intercal}$ and all the other parameters and metrics are kept same as in the 2×2 MIMO case.

It is obvious from the system model of 4×4 LoS MIMO that there are 4^4 noise-free outputs that need to be considered for quantizer design and it is, consequently, not easy to perform the similar analysis that we perform for 2×2 MIMO. For that reason, we rely on the probability density functions of the outputs before quantization and design the regular quantizers based on those. Due to the symmetry, it is clear that the outputs before quantization (i.e., $\{Y_i\}_{i=1}^4$) have the same probability density function. Hence, without loss of generality, we focus on one of the outputs before quantization (e.g., Y_1) to design the corresponding quantizer and employ the same quantizer for all outputs. To begin with, Y_1 has a complex distribution and it is difficult to specify the quantizer regions by considering that. In order to facilitate it, first, we approximate it with a circularly-symmetric complex Gaussian distribution; that is, $\tilde{Y} \sim \mathcal{CN}(0, \tilde{\sigma}^2)$ where we set $\tilde{\sigma}^2 = \mathbb{E}\{Y_1\, Y_1^{\dagger}\}$ in order to minimize Kullback-Leibler divergence between the distributions of Y_1 and $\tilde{Y}$. Then, we obtain the quantizers by considering that Gaussian approximation.

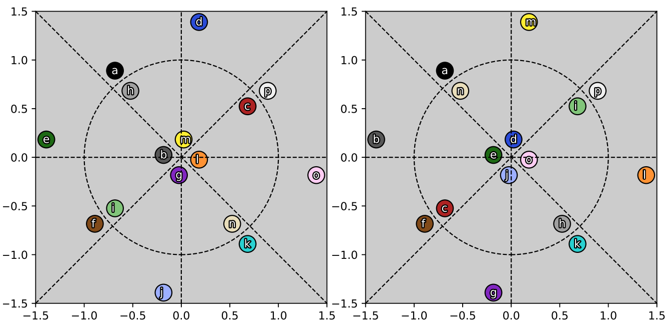

Fig. 4. All possible noise-free outputs before the quantization, $e^{j\phi}(X_1 + e^{j\theta}X_2)/\sqrt{2}$ (Left) and $e^{j\phi}(e^{j\theta}X_1 + X_2)/\sqrt{2}$ (Right), for $\theta = 5\pi/12$ and $\phi = \pi/4$.

In the quantizer design of 4×4 MIMO, we mainly consider two different regular quantization schemes, I/Q quantization and amplitude/phase quantization, each having a total of 16 regions as in Fig. 3. In consideration of those two schemes, we determine the quantizer regions based on two different metrics: equal probability-based regions and minimum mean squared quantization error (MMSQE)-based regions. The former is obtained by partitioning the fitted complex Gaussian distribution into equal probability regions, whereas the latter is derived by minimizing the distortion measured conventionally by mean squared error.

VI. Numerical Results

In this section, numerical examples are provided to illustrate the theoretical results. First, the statements in the lemmas and the propositions are exemplified based on the noise-free outputs (i.e., the outputs as $\sigma \to 0$) before quantization and then the Shannon limits for different quantization schemes are compared.

We illustrate the geometry behind the proofs by presenting noiseless outputs prior to quantization for a well-conditioned and a poorly conditioned channel in Fig. 4 and Fig. 5, respectively. We see that some output pairs (e.g., (b, e), (d, m), (g, j) and (l, o) in Fig. 4 and (b, o), (d, g), (e, l) and (j, m) in Fig. 5)

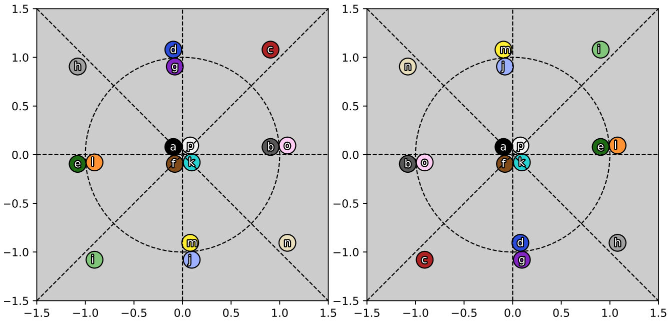

Fig. 5. All possible noise-free outputs before the quantization, $e^{j\phi}(X_1 + e^{j\theta}X_2)/\sqrt{2}$ (Left) and $e^{j\phi}(e^{j\theta}X_1 + X_2)/\sqrt{2}$ (Right), for $\theta = 17\pi/18$ and $\phi = \pi/18$.

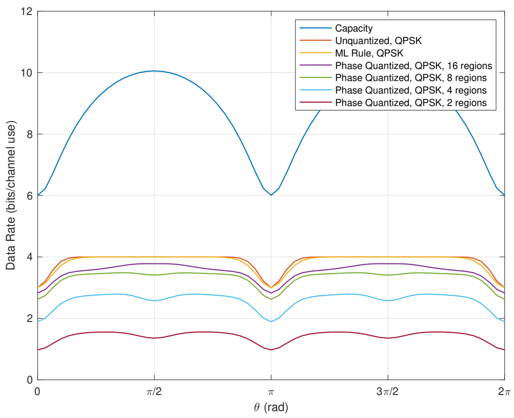

Fig. 6. Data rate versus θ for various scenarios including the phase-only quantization schemes with different number of regions, where SNR is 15 dB.

have the same phase at *both* receive antennas, and hence cannot be distinguished based on phase-only quantization, as stated in Lemma 1. On the other hand, the other outputs can indeed be distinguished based on phase-only quantization. In addition, for given θ and ϕ, the phase of noise-free outputs can have 8 different values, and two different outputs having two different phase values cannot be in the same bin for phase-only quantization with 8 equal sectors. This is the intuitive basis for Proposition 2. Lastly, noise-free output pairs having the same phase at both receive antennas, such as (b, e) in Fig. 4 can be separated by employing an amplitude quantization scheme with 2 regions as illustrated in Fig. 4 and Fig. 5. This is the intuition behind Proposition 3.

Next, we plot the data rate (mutual information) attained by different quantization schemes. Two benchmarks are considered: an unquantized system, and a quantizer based on Voronoi regions to separating the outputs at each antenna. We may view the latter as an ML decision rule at each antenna, where input-pairs that fall on top of each other are interpreted as a single point, and it is easy to see that it attains the unquantized benchmark at high SNR. However, it depends on θ and Φ, and is an irregular quantizer that is unattractive in practice.

Fig. 6 and Fig. 8 plot data rate versus $\theta \in [0, 2\pi)$ at 15 dB SNR for phase-only and amplitude-phase quantization,

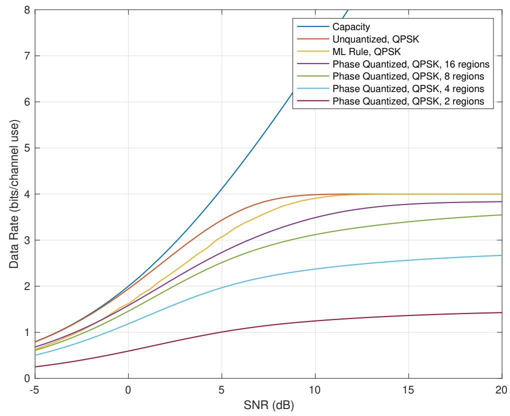

Fig. 7. Data rate versus SNR for various scenarios including the phase-only quantization schemes with different number of regions, where $\theta = \pi/2$.

respectively. Similarly, Fig. 7 and Fig. 9 plot data rates versus SNR, fixing $\theta = \pi/2$ (the best conditioned channel). For 2-level amplitude and 8-level phase quantization, the amplitude threshold is set to $A_1 = 1$, whereas the thresholds are $A_1 = 0.75$ and $A_2 = 1.25$ for 3-level amplitude and 8-level phase quantization. The plots illustrate the trends predicted by our theoretical results: phase-only quantization does not attain the unquantized or ML benchmarks, while amplitude-phase quantization does attain these at high enough SNR. However, there are some differences between performance at moderate SNR and high-SNR asymptotics. While 8 phase quantization bins are as good as any other phase-only quantization scheme asymptotically, using 16 quantization bins does provide better performance at moderate SNRs (Fig. 6 and Fig. 7). Similarly, while 2-level amplitude quantization suffices, there is a gain at moderate SNRs with 3-level quantization (Fig. 8 and Fig. 9). In particular, Fig. 9 shows that for a well-conditioned channel, while 2-level amplitude quantization attains the unquantized benchmark at high enough SNR, 3-level amplitude quantization has a significant advantage at moderate SNRs, reaching unquantized performance at around 12.5 dB.

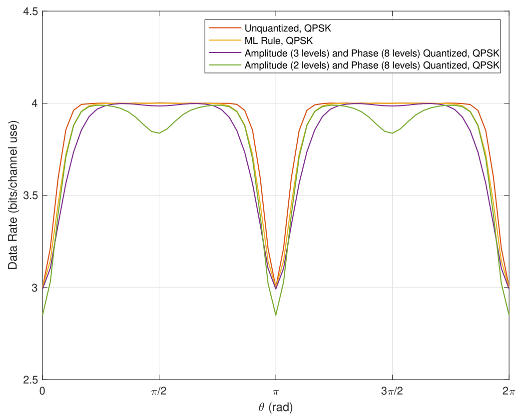

Fig. 8. Data rate versus θ for various scenarios including the amplitude and phase quantization schemes with different number of regions, where SNR is 15 dB.

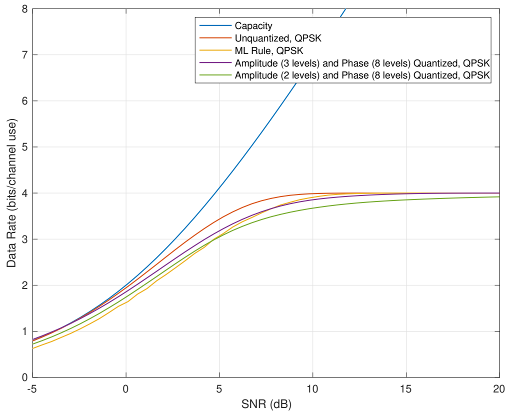

Fig. 9. Data rate versus SNR for various scenarios including the amplitude and phase quantization schemes with different number of regions, where $\theta = \pi/2$.

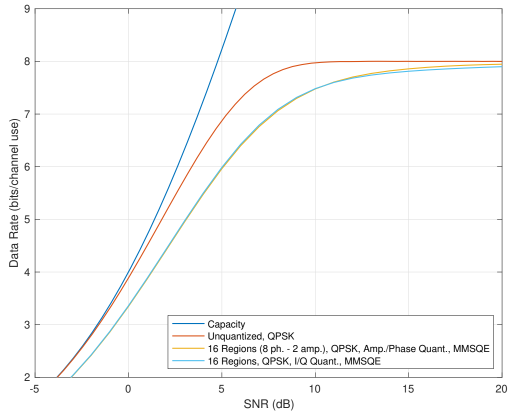

Fig. 11. Data rate versus SNR for MMSQE-based quantization scenarios of 4×4 MIMO.

Fig. 10 and Fig. 11 plot data rates versus SNR, setting $\theta = \pi/2$, for different quantization scenarios of 4×4 LoS MIMO. The plots show that I/Q quantization outperforms amplitude/phase quantization when the equal probability regions are taken into account for quantizer design. Also, conventional MMSQE-based quantizer cannot achieve better than the equal probability quantizer when I/Q quantization is considered as a quantization scheme. Fig. 10 illustrates that equal probability I/Q quantization having 16 regions attains the maximum data rate of 8 bits per channel use at around 15 dB.

VII. Conclusion

Our results employ geometric insights for simple channels and small constellations, with high-SNR asymptotics serving as a useful alternative to brute force optimization. An interesting open question is to investigate how far this approach can be pushed as we increase the number of spatial channels and the constellation size, and as we incur dispersion due to geometric misalignments such as those considered in [7], [10].

Acknowledgment

This work was supported in part by ComSenTer, one of six centers in JUMP, a Semiconductor Research Corporation (SRC) program sponsored by DARPA. Use was made of computational facilities purchased with funds from the National Science Foundation (CNS-1725797) and administered by the Center for Scientific Computing (CSC). The CSC is supported by the California NanoSystems Institute and the Materials Research Science and Engineering Center (MRSEC; NSF DMR 1720256) at UC Santa Barbara.

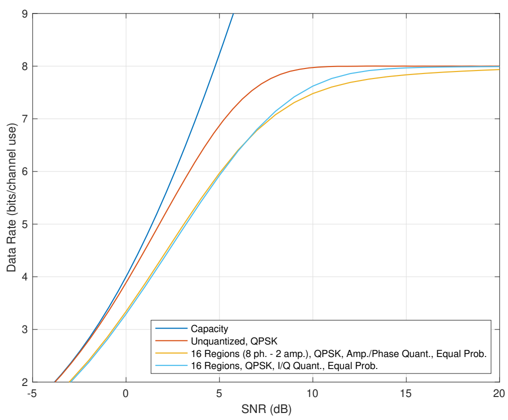

Fig. 10. Data rate versus SNR for equal probability-based quantization scenarios of 4×4 MIMO.

References

[1] R. H. Walden, "Analog-to-digital converter survey and analysis," *IEEE Journal on Selected Areas in Communications*, vol. 17, no. 4, pp. 539–550, Apr. 1999.

[2] E. Torkildson, U. Madhow, and M. Rodwell, "Indoor millimeter wave MIMO: Feasibility and performance," *IEEE Transactions on Wireless Communications*, vol. 10, no. 12, pp. 4150–4160, Dec. 2011.

[3] J. Singh, O. Dabeer, and U. Madhow, "On the limits of communication with low-precision analog-to-digital conversion at the receiver," *IEEE Transactions on Communications*, vol. 57, no. 12, pp. 3629–3639, Dec. 2009.

[4] J. Mo and R. W. Heath, "Capacity analysis of one-bit quantized MIMO systems with transmitter channel state information," *IEEE Transactions on Signal Processing*, vol. 63, no. 20, pp. 5498–5512, Oct. 2015.

[5] A. Khalili, S. Rini, L. Barletta, E. Erkip, and Y. C. Eldar, "On MIMO channel capacity with output quantization constraints," in *IEEE International Symposium on Information Theory (ISIT)*, June 2018, pp. 1355–1359.

[6] C. Sheldon, M. Seo, E. Torkildson, U. Madhow, and M. Rodwell, "A 2.4 Gb/s millimeter-wave link using adaptive spatial multiplexing," in *IEEE Antennas and Propagation Society International Symposium*, July 2010, pp. 1–4.

[7] M. Sawaby, B. Mamandipoor, U. Madhow, and A. Arbabian, "Analog processing to enable scalable high-throughput mm-Wave wireless fiber systems," in *50th Asilomar Conference on Signals, Systems and Computers*, Nov. 2016, pp. 1658–1662.

[8] O. Dabeer and U. Madhow, "Channel estimation with low-precision analog-to-digital conversion," in *IEEE International Conference on Communications (ICC)*, May 2010, pp. 1–6.

[9] C. Stöckle, J. Munir, A. Mezghani, and J. A. Nossek, "Channel estimation in massive MIMO systems using 1-bit quantization," in *IEEE 17th International Workshop on Signal Processing Advances in Wireless Communications (SPAWC)*, July 2016, pp. 1–6.

[10] P. Raviteja and U. Madhow, "Spatially oversampled demultiplexing in mmWave LoS MIMO," in *IEEE 19th International Workshop on Signal Processing Advances in Wireless Communications (SPAWC)*, June 2018, pp. 1–5.